JB Accepted Manuscript Posted Online 8 August 2016
J. Bacteriol. doi:10.1128/JB.00451-16

Lipogenesis and redox balance in nitrogen-fixing pea bacteroids

Jason J. Terpolilli[a,b], Shyam, K. Masakapalli[c], Ramakrishnan Karunakaran[b], Isabel Webb[b,c], Rob Green[b], Nicholas J. Watmough[d], Nicholas J. Kruger[c], R. George Ratcliffe[c], Philip S. Poole[b,c,d#]

Centre for Rhizobium Studies, Murdoch University, Perth, Australia[a]; Department of Molecular Microbiology, John Innes Centre, Norwich, United Kingdom[b]; Department of Plant Sciences, University of Oxford, United Kingdom[c]; Centre for Molecular Structure and Biochemistry, University of East Anglia, United Kingdom[d]; Sir Walter Murdoch Adjunct Professor, Murdoch University, Perth, Australia[e]

Running Head: Lipogenesis and redox in N_2-fixing pea bacteroids

[#]Address correspondence to Philip S. Poole, philip.poole@plants.ox.ac.uk

Abstract

Within legume root nodules, rhizobia differentiate into bacteroids that oxidise host-derived dicarboxylic acids, which is assumed to occur via the TCA-cycle to generate NAD(P)H for reduction of N_2. Metabolic flux analysis of laboratory grown *Rhizobium leguminosarum* showed that the flux from ^{13}C-succinate was consistent with respiration of an obligate aerobe growing on a TCA-cycle intermediate as the sole carbon source. However, the instability of fragile pea bacteroids prevented their steady state labelling under N_2-fixing conditons. Therefore, comparitive metabolomic profiling was used to compare free-living *R. leguminosarum* with pea bacteroids. While the TCA-cycle was shown to be essential for maximal rates of N_2-fixation, pyruvate (5.5-fold down), acetyl-CoA (50-fold down), free coenzyme A (33-fold) and citrate (4.5-fold down) were much lower in bacteroids. Instead of completely oxidising acetyl-CoA, pea bacteroids channel it into both lipid and the lipid-like polymer poly-β-hydroxybutyrate (PHB), the latter via a type II PHB synthase that is only active in bacteroids. Lipogenesis may be a fundamental requirement of the redox poise of electron donation to N_2 in all legume nodules. Direct reduction by NAD(P)H of the likely electron donors for nitrogenase, such as ferredoxin, is inconsistent with their redox potentials. Instead, bacteroids must balance the production of NAD(P)H from oxidation of acetyl-CoA in the TCA-cycle with its storage in PHB and lipids.

Importance

Biological nitrogen fixation by symbiotic bacteria (rhizobia) in legume root nodules is an energy-expensive process. Within legume root nodules, rhizobia differentiate into bacteroids that oxidise host-derived dicarboxylic acids, which is assumed to occur via the TCA-cycle to generate NAD(P)H for reduction of N_2. However, direct reduction of the likely

electron donors for nitrogenase, such as ferredoxin, is inconsistent with their redox potentials. Instead bacteroids must balance oxidation of plant-derived dicarboxylates in the TCA-cycle with lipid synthesis. Pea bacteroids channel acetyl-CoA into both lipid and the lipid-like polymer poly-β-hydroxybutyrate, the latter via a type II PHB synthase. Lipogenesis is likely to be a fundamental requirement of the redox poise of electron donation to N_2 in all legume nodules.

Introduction

Biological reduction (or fixation) of atmospheric nitrogen (N_2) to ammonia (NH_3) provides up to 50% of the biosphere's available nitrogen, mostly through symbioses between soil bacteria (rhizobia) and legumes (1, 2). These symbioses are initiated by rhizobia infecting legume roots, resulting in the formation of nodules. Rhizobia differentiate into N_2-fixing bacteroids that express nitrogenase to reduce N_2 to NH_3 under microaerobic conditions (3). Bacteroids receive carbon from the legume while secreting NH_3 to the plant. The overall stoichiometry of N_2 fixation under ideal conditions is:

$$N_2 + 8e^- + 8H^+ + 16ATP \longrightarrow 2NH_3 + H_2 + 16ADP + 16P_i \quad (1)$$

Thus, eight moles of electrons and protons and 16 moles of ATP reduce a single mole of N_2, making N_2 fixation energetically expensive.

Legumes energise bacteroid N_2 fixation by supplying dicarboxylates, principally malate (4), which must be oxidised to yield ATP and electrons to reduce N_2. Bacteroids metabolise malate by NAD^+-dependent malic enzyme (5-7) and pyruvate dehydrogenase to provide acetyl-CoA, which can be completely oxidised in the TCA-cycle, yielding $FADH_2$ and NAD(P)H. The standard model is that NAD(P)H supplies electrons both to nitrogenase via ferredoxin,

or an equivalent low potential electron donor, and to an electron transport chain for ATP synthesis (8, 9).

This is supported by work in *Rhizobium leguminosarum* and *Sinorhizobium meliloti*, where TCA-cycle mutants are unable to fix N_2 in symbiosis with pea (*Pisum sativum*) and alfalfa (*Medicago sativa*), respectively (10-13). However, the TCA-cycle provides both reductant and biosynthetic precursors, so the abolition of N_2 fixation in these mutants could be due to insufficient NAD(P)H to directly power nitrogenase or, equally, result from biosynthetic deficiencies. In contrast, in soybean (*Glycine max*) bacteroids, the TCA-cycle is either dispensable for N_2 fixation or can be bypassed, with isocitrate dehydrogenase and 2-oxoglutarate dehydrogenase mutants of *Bradyrhizobium japonicum* able to fix N_2 at wild-type rates (14, 15). Moreover, standard midpoint potentials indicate that NAD(P)H is unlikely to donate electrons directly to ferredoxin [$E^{0'}$ for NAD^+/NADH is -320 mV, $NADP^+$/NADPH is -324 mV and ferredoxin (Fe^{3+}/Fe^{2+}) is -484 mV] (16, 17). Thus some other, as yet undefined mechanism, must exist to transfer electrons to nitrogenase in root nodule bacteroids.

Finally, N_2-fixing bacteroids in nodules formed by soybean and common bean (*Phaseolus vulgaris*) accumulate large quantities of the lipid-like polymer poly-β-hydroxybutyrate (PHB), while bacteroids from pea, alfalfa and clover (*Trifolium spp.*) apparently do not (18). While abolishing PHB synthesis does not adversely affect N_2 fixation rates in soybean and common bean (19-21), in *Azorhizobium caulinodans*, mutation of PHB synthase prevents N_2 fixation in both free-living and symbiotic forms (22), implying a fundamental role for PHB synthesis in at least some N_2-fixing rhizobia.

96

97 Determining how N_2 is fixed by bacteroids, arguably the second most important nutrient
98 assimilation cycle after photosynthesis, requires an understanding of bacteroid carbon
99 metabolism. Metabolic profiling, flux analysis, as well as mutational and N_2 fixation studies
100 were used to investigate carbon flow in bacteroids. Remarkably, this reveals that the TCA-
101 cycle is not the only sink for plant-derived carbon in symbiotic N_2 fixation; rather, pea
102 bacteroids divert appreciable quantities of acetyl-CoA into the production of lipid or PHB.
103 N_2-fixing bacteroids are therefore inherently lipogenic and this is probably a metabolic
104 requirement for N_2 fixation.

105

106 **Materials and Methods**

107 **Bacterial strains and culture conditions.** Bacterial strains and plasmids used in this study are
108 detailed in Table 1. *Rhizobium leguminosarum* bv. viciae (Rlv3841) was grown at 28°C on
109 tryptone yeast extract (TY) (23) or acid minimal salts medium (AMS)(24) with succinate (20
110 mM) and NH_4Cl (10 mM) as the sole carbon and nitrogen source, respectively. Where
111 appropriate, antibiotics were used at the following concentrations (in μg ml^{-1}): streptomycin
112 (500), neomycin (80), spectinomycin (50), gentamycin (20) and ampicillin (50).

113

114 **Metabolic flux analysis.** Rlv3841 cells grown in succinate/NH_4Cl AMS were harvested at
115 mid-log phase (OD_{600} ≈ 0.5) and subcultured into fresh AMS media to a starting OD_{600} of
116 0.02, with 20 mM [$^{13}C_4$]succinate (20% fractional abundance). Cells were harvested at OD_{600}
117 of 0.3 and centrifuged at 8,500 x g for 5 min. The resulting pellet was washed with fresh
118 AMS, centrifuged and the resulting cell pellet was extracted in 80% (v/v) ethanol at 80°C for
119 5 min, prior to centrifugation at 12,000 x g for 5 min. The supernatant containing the soluble

amino acids, organic acids and sugars was dried by vacuum centrifugation. The insoluble pellet was rapidly frozen in liquid N_2 and freeze-dried. Protein in the insoluble fraction was hydrolysed to its component amino acids by incubation with 6 M HCl for 24 h at 100°C.

GC-MS analysis of derivatised amino acids, organic acids and sugars was performed on an Agilent 7890A GC/5975C quadrupole MS system as described elsewhere (25). Amino acids and organic acids were analysed after derivatisation using *N*-*tert*-butyldimethylsilyl-*N*-methyltrifluoroacetamide (MTBSTFA) or *N*-methyl-*N*-(trimethylsilyl)-trifluroacetamide (MSTFA); sugars were treated with methoxyamine hydrochloride and then derivatised with MSTFA. Protein-derived and soluble amino acids were examined separately. Mass isotopomer abundances were quantified using Chemstation and corrected for the presence of naturally occurring heavy isotopes introduced during derivatisation. The chemical fragments used for metabolic flux analysis are detailed in Supplementary Table 1.

Metabolic modelling was performed with 13C-FLUX (version 20050329) using the iterative procedure described before (25, 26). A complete description of the model, which also defines the network carbon atom transitions, is provided in Supplementary Table 2 and net fluxes are provided in Supplementary Table 3. During initial parameter fitting, fluxes to biomass outputs were allowed to vary, and the mean values from ten best-fit estimates were then used to constrain the network output flux values in subsequent simulations. Malate and oxaloacetate were combined into a single metabolite pool, as were phosphoenolpyruvate and pyruvate, to improve determinability of fluxes between these intermediates. No adjustments were required to compensate for the contribution of pre-

143 existing unlabelled pools of metabolites. Molar fluxes are reported relative to a succinate
144 uptake flux of 1.
145
146 **Material for metabolite profiling.** To prepare samples of free-living Rlv3841, six
147 independent cultures of Rlv3841, derived from six isolated colonies of the strain, were
148 grown in AMS on a gyratory shaker at 250 rpm to an OD_{600} of 0.4. Cell pellets were collected
149 by centrifugation (5000 x g, 5 min), washed with isolation buffer (8 mM K_2HPO_4, 2 mM
150 KH_2PO_4, 2 mM $MgCl_2$) and stored at -80°C for later use in metabolite profiling.
151
152 To prepare bacteroid and nodule cytosolic samples, seeds of *P. sativum* cv. Avola were
153 surfaced sterilised with 70% (v/v) ethanol for 30 s, rinsed once in sterile water and then
154 immersed in a 2% (w/v) NaOCl solution for 2 min, prior to rinsing 10 times in sterile water.
155 Seeds were sown into 2 L beakers containing washed and autoclaved fine grade vermiculite.
156 Six independent cultures of the test strains Rlv3841 or RU116, derived from six isolated
157 colonies of each strain, were prepared. A one ml aliquot of each culture was inoculated into
158 a minimum of six pots, at cell densities between 5-9 x 10^7 cells ml^{-1}. Seeds were initially
159 sown in duplicate and thinned to one plant per pot after seven days. Plants were watered
160 once with 250 ml nitrogen-free nutrient solution as previously described (24) and were
161 incubated in an illuminated environment-controlled growth room at 22°C on a 16 h day, 8 h
162 night cycle.
163
164 Plants were harvested at 28 days post-inoculation (dpi) for metabolomic profiling.
165 Approximately 1.5 g of nodule tissue was excised from plants from each set of pots. Nodules
166 were ground in isolation buffer (8 mM K_2HPO_4, 2 mM KH_2PO_4, 2 mM $MgCl_2$) and the

167 homogenate was passed through muslin and centrifuged (250 x g for 5 min) to remove plant
168 debris before a further round of centrifugation (5000 x g, 10 min) to pellet the bacteroids.
169 The resulting supernatant, representing the nodule cytosol fraction, was freeze-dried and
170 the pellet, representing the bacteroid fraction, was washed twice with isolation buffer,
171 centrifuged (5000 x g, 10 min) and the pellets frozen at -80°C for later use in metabolite
172 profiling.

173 **Metabolite profiling platform.** Metabolomic profiles of free-living, bacteroid and nodule
174 cytosol were each performed using non-biased, global metabolome profiling technology
175 based on GC/MS and UHLC/MS/MS^2 platforms (27, 28) developed by Metabolon
176 (www.metabolon.com). Six replicate samples from each treatment (free-living, bacteroid
177 and nodule cytosol) were extracted using the automated MicroLab STAR® system (Hamilton,
178 www.hamiltoncompany.com). Recovery standards were added prior to the first step in the
179 extraction process for quality control purposes. To monitor total process variability a series
180 of technical replicates were taken from a pool made from small aliquots of all the
181 experimental samples. These were spaced evenly among the randomly ordered
182 experimental samples and all consistently detected metabolites were monitored for
183 reproducibility. Sample preparation was conducted using methanol extraction to remove
184 the protein fraction while allowing maximum recovery of small molecules. The resulting
185 extract was divided into two fractions; one for analysis by LC and one for analysis by GC.
186 Samples were placed briefly on a TurboVap® (Zymark) to remove the organic solvent. Each
187 sample was frozen and dried under vacuum. Samples were then prepared for the
188 appropriate instrument, either LC/MS or GC/MS.

189

190 The LC/MS portion of the platform was based on a Waters ACQUITY UHPLC and a Thermo-
191 Finnigan LTQ mass spectrometer, which consisted of an electrospray ionization source and
192 linear ion-trap mass analyser. The sample extract was split into two aliquots, dried, then
193 reconstituted in acidic or basic LC-compatible solvents, each of which contained 11 or more
194 injection standards at fixed concentrations. One aliquot was analysed using acidic positive
195 ion optimized conditions and the other using basic negative ion optimized conditions in two
196 independent injections using separate dedicated columns. Extracts reconstituted in acidic
197 conditions were gradient-eluted using water and methanol both containing 0.1% (v/v)
198 formic acid, while the basic extracts, which also used water/methanol, contained 6.5 mM
199 NH_4HCO_3. The MS analysis alternated between MS and data-dependent MS/MS scans using
200 dynamic exclusion.
201
202 The samples destined for GC/MS analysis were re-dried under vacuum desiccation for a
203 minimum of 24 h prior to being derivatised under dried N_2 using bistrimethyl-silyl-
204 triflouroacetamide (BSTFA). The GC column was 5% phenyl and the temperature ramp was
205 40°C to 300°C, over a 16 min period. Samples were analysed on a Thermo-Finnigan Trace
206 DSQ fast-scanning single-quadrupole gas chromatograph mass spectrometer using electron
207 impact ionization.
208
209 **Compound identification, data handling and statistical analysis.** For metabolite profiling,
210 identification of known chemical entities was based on comparison to metabolomic library
211 entries of purified standards as previously described (28, 29). Statistical analysis was
212 performed using the software packages Array Studio (Omicsoft) and R (http://www.r-
213 project.org/). Where a given metabolite was not detected in a particular sample, then the

observed minimum detected value for that metabolite from the analysis was assigned, under the assumption that missing values were not random, but resulted from the compound being below the limit of detection. Data for free-living and bacteroid samples were then normalised to protein content, as determined by Bradford assay(30). For the comparison of the bacteroids to the nodule cytosol, normalisation was performed by extracting proportional amounts of bacteroid and cytosolic fractions of matched starting samples. That is, the total yield of bacteroid and cytosolic fractions for each sample was known, and a constant percentage of each fraction was analysed in order to compare relative amounts of metabolites in each fraction. The statistical model utilized the matched pair nature of the samples to account for absolute differences between the samples. Welch's two-sample *t*-test was used to identify metabolites that differed significantly between experimental groups ($P < 0.05$) and the false discovery rate (FDR) was also calculated(31) to account for the multiple comparisons that normally occur in metabolomic-based studies ($Q < 0.1$). Thus, metabolites were considered to be significantly different if they met the criteria $P < 0.05$ and $Q < 0.10$.

Assessment of N_2 fixation. Plants for assessment of N_2 fixation were grown as described above in "Material for metabolite profiling", with the following exceptions. For measurement of N_2 fixation by acetylene reduction assay, plants were grown in 1 L pots and harvested at the onset of flowering (21 dpi). Whole plants were removed from growth pots and transferred to 250 ml sealed bottles. When rates of acetylene reduction of detached nodules were measured, nodules were excised and immediately transferred into a 25 ml bottle and assayed. Rates of N_2 fixation were determined by the amount of acetylene reduced after 1 h in an atmosphere consisting of 95% air-5% acetylene, as previously

described (32). Following the acetylene reduction assay, bacteroid protein was quantified by excising nodules from roots and grinding in 40 mM HEPES (pH 7.0). The homogenate was passed through muslin and the eluate centrifuged (250 x g for 5 min) to remove plant debris. The supernatant was then centrifuged (5000 x g, 10 min) to pellet the bacteroids. Bacteroids were lysed by two rounds of ribolysing on a Fast Prep Ribolyser FP120 (BIO101/Savant) at a setting of 6.5 for 30 s, with samples on ice for 5 min in between. The protein content in the resulting supernatant was determined by Bradford assay (30) using the Pierce Coomassie assay kit (Pierce, cat# 23200) with BSA as the protein standard.

For assessment of N_2 fixation by plant biomass accumulation, plants were grown in 2 L pots and were supplied with 200 ml of additional sterile water at 28 dpi. Plants were then harvested at 47 dpi by cutting shoots below the hypocotyl and drying at 60°C for 48 h prior to weighing.

Lipid analysis. Bacteroids for lipids analysis were collected from nodules harvested from plants grown as described in the material for metabolite profiling section and harvested at 28 dpi. Nodules were ground in 20 mM HEPES buffer (pH 7.0) and purified by Percoll gradient (33). Cells of free-living Rlv3841 were grown in AMS with succinate and NH_4Cl and harvested at OD_{600} 0.4-0.6 by centrifugation (5000 x g for 10 min). Resultant bacteroid and cell pellets were stored at -80°C for later use. Bacteroid and cell pellets were lysed by ribolyser as described above and centrifuged (10,000 x g for 10 min). The supernatant was then centrifuged (20,000 x g for 20 min), prior to further ultracentrifugation (60,000 x g for 60 min) to remove cell membranes. The supernatant was concentrated by vacuum centrifugation prior to lipid quantification using the triglyceride determination kit (Sigma,

cat# TR0100). Protein determination was performed using the Bradford assay as described above.

Mutant construction and phenotyping. To construct the *phaC2* (pRL100105) mutant of Rlv3841, primers pr1645 and pr1646 (see Supplementary Table 1) were used to amplify a 2.8 Kb of the region containing the gene and the PCR product was cloned into pJET1.2/blunt, giving plasmid pLMB834. The Ω-streptomycin/spectinomycin cassette from pHP45-ΩSmSp was cloned into the unique *Eco*RI site of pLMB834, to produce pLMB835. The BglII fragment from pLMB835 was cloned into pJQ200SK to produce pLMB839. Plasmid pLMB839 was then conjugated into strain Rlv3841, using pRK2013 as a helper plasmid, to produce *phaC2* mutants as previously described(5) resulting in LMB814. The mutation was confirmed by PCR mapping using primer pairs pr1648-potfarforward and pr1657-potfarforward. Strain LMB816, the *phaC1* (RL2098) *phaC2* (pRL100105) double mutant, was made by using the general transducing phage RL38 to lyse strain RU137. The kanamycin-marked *phaC1*::Tn5 mutation was then back-transduced into LMB814 to generate LMB816, as previously described (34) and the mutation was confirmed by PCR mapping with pr1647-potfarforward, pr1648-potfarforward and pr1647-Tn*5*-1 primer pairs. Assessment of N_2 fixation of the resulting mutants was performed as described above. Transmission electron microscopy was performed on nodules harvested from plants at 28 dpi and the methods for nodule sectioning, staining and microscopy are as detailed previously (20).

Results

285 **Metabolic flux analysis of free-living rhizobia.** Dicarboxylates are provided to bacteroids by
286 plants to support N_2 fixation (3, 4), so the pathways operating in free-living *Rhizobium*
287 *leguminosarum* bv. viciae 3841 (Rlv3841) growing on [$^{13}C_4$] succinate were quantified. The
288 major flux of succinate metabolism in Rlv3841 was via fumarate to malate (Figure 1) and
289 subsequently from malate to pyruvate and oxaloacetate to phosphoenolpyruvate. These
290 fluxes would support the major metabolic requirements of cells growing on a TCA-cycle
291 intermediate for synthesis of acetyl-CoA to supply the TCA-cycle and phosphoenolpyruvate
292 for biosynthesis of sugars. Large fluxes were also detected in gluconeogenesis converting
293 phosphoenolpyruvate to triose phosphates, in the oxidative decarboxylation of pyruvate to
294 acetyl-CoA and in the TCA-cycle from oxaloacetate to 2-oxoglutarate. Overall, these fluxes
295 are consistent with respiration of an obligate aerobe growing on a TCA-cycle intermediate
296 as the sole carbon source.
297
298 Currently, metabolic flux analysis cannot be conducted on notoriously fragile isolated pea
299 bacteroids (35). Nitrogenase activity, as measured by acetylene reduction, in isolated pea
300 nodules collapsed 90 minutes after excision to less than 2% of that in nodules on roots (0.25
301 ± 0.03 *vs* 18.3 ± 2.5 nmol acetylene reduced. mg nodule^{-1}. h^{-1}). This precludes labelling of
302 nodule metabolites to isotopic steady state under physiologically relevant conditions in an
303 isolated system. Moreover, the likely slow rate of protein turnover in non-dividing
304 bacteroids compromises the use of the labelling patterns of protein-derived amino acids to
305 reflect those of their metabolic precursors. We therefore used metabolite profiling to
306 examine the differences in levels of metabolic intermediates between cultured cells and
307 bacteroids.
308

309 **Bacteroid Central Metabolism.** The metabolic profiles of free-living and bacteroid forms of
310 Rlv3841 were analysed using non-biased, untargeted metabolome analysis (27, 28).
311 Metabolites most highly elevated in bacteroids relative to free-living Rlv3841 were
312 homoserine and asparagine (increased 105- and 58-fold respectively; Figure 2). Both were
313 also high in the nodule cytosolic fraction relative to bacteroids (33- and 11-fold increased,
314 Supplementary Table 5), in accordance with previous observations (36, 37), and consistent
315 with their known plant origin. Asparagine is made in the plant cytosol as the primary
316 nitrogen export product from nodules (35). Furthermore, free asparagine is not made by
317 Rlv3841, which from analysis of its genome uses the GatCAB pathway to insert asparagine
318 into proteins by charging asparaginyl-tRNA with aspartate and then transamidating
319 aspartate to asparagine (38). In addition, catabolism of asparagine and homoserine is not
320 up-regulated in bacteroids (39), nor do catabolic mutants show reduced N_2 fixation rates
321 (40, 41), consistent with minor roles in symbiosis.
322
323 Our fundamental question is whether the TCA-cycle is altered during symbiotic N_2 fixation.
324 The dicarboxylates malate, fumarate and succinate are the carbon sources for bacteroids *in*
325 *planta* and levels of all three were increased in bacteroids relative to free-living cells (Figure
326 2). Moreover, these metabolites were also much higher in the plant nodule cytosol fraction
327 relative to bacteroids (malate 14-, fumarate 20-; succinate 2.5-fold, Supplementary Table 5),
328 consistent with active plant dicarboxylate synthesis.
329
330 Metabolism of dicarboxylates by bacteroids is via malic enzyme and phosphoenolpyruvate
331 carboxykinase to pyruvate and phosphoenolpyruvate, respectively, with pyruvate
332 subsequently oxidatively decarboxylated to acetyl-CoA (5-7). The intermediates of sugar

333 metabolism such as 3-phosphoglycerate, fructose-6-phosphate and glucose-6-phosphate
334 and the pentose phosphate pathway (ribulose-5-phosphate and xylulose-5-phosphate) were
335 greatly reduced (Figure 2), suggesting little sugar synthesis occurs in bacteroids.
336 Remarkably, pyruvate (5.5-fold down), acetyl-CoA (50-fold down), free coenzyme A (33-fold)
337 and citrate (4.5-fold down) were much lower in bacteroids (Figure 2). In sharp contrast, the
338 transcription and enzymatic activity of citrate synthase (RL2234, *icdB*) was increased 3.2-
339 and 12-fold, respectively and increases in the activity and transcription of other enzymes of
340 the decarboxylating arm of the TCA-cycle have been noted (39, 42). While such increased
341 enzyme biosynthesis might indicate increased flux into the TCA-cycle, it is equally consistent
342 with lower feedback inhibition of the synthesis and activity of enzymes by key intermediates
343 such as acetyl-CoA and citrate (43, 44).
344
345 Carbon in the TCA cycle could also be channelled to glutamate, which is synthesised from 2-
346 oxoglutarate by glutamine synthetase/glutamate synthase (GS/GOGAT)(45). However,
347 glutamate levels were 20-fold lower in bacteroids relative to free living cells (Figure 2),
348 consistent with GS/GOGAT activity being both low and not essential in mature bacteroids
349 (46). Metabolites derived from glutamate, including glutathione and N-acetylglutamate
350 were also reduced while levels of many other amino acids were either only slightly altered
351 or unchanged in bacteroids (Figure 2).
352
353 However, steady state metabolite levels do not represent flux. Low levels of pyruvate,
354 acetyl-CoA, coenzyme A and citrate in bacteroids may indicate a low rate of synthesis but
355 can equally result from rapid turnover. Furthermore, metabolites may dramatically change
356 concentrations during isolation of bacteroids from nodules. We addressed this by comparing

wild-type with mutant bacteroids defective in the TCA-cycle, which should lead to different metabolite profiles. If low acetyl-CoA in wild-type bacteroids relative to free-living cells results from increased flux through the TCA-cycle, then TCA-cycle mutants should have elevated acetyl-CoA.

Metabolite profile of a TCA cycle mutant. We previously isolated several Tn*5* insertions in Rlv3841 genes encoding TCA-cycle enzymes (12). Malate dehydrogenase, succinyl-CoA synthetase and the E1 and E2 components of the 2-oxoglutarate dehydrogenase complex are transcribed from the *mdh-sucCDAB* operon (47). Mutations in *sucA* (RU156, RU724 and RU733) or *sucB* (RU726), encoding the E1 and E2 components of the 2-oxoglutarate dehydrogenase complex, respectively abolished 2-oxoglutarate dehydrogenase activity (12), resulting in plants that failed to reduce acetylene (Fix^-). Therefore, blocking the TCA-cycle in Rlv3841 prevents N_2 fixation. However, strain RU116, mutated in *sucD* (encoding the β-subunit of succinyl-CoA synthetase), originally scored as Fix^- based on yellowing of plants and small nodules but retaining low levels of succinyl-CoA synthetase activity (12), we now show is able to reduce acetylene at 35% of the wild-type rate (Figure 3). This mutation may affect the number of bacteroids in nodules, total nodule mass or reduce nitrogenase activity. However, acetylene reduction per unit bacteroid protein and shoot dry matter of plants grown in nitrogen-free conditions inoculated with the *sucD* mutant were 45%- and-51% of the wild-type values, respectively (Figure 3). Therefore, *sucD* bacteroids have lowered N_2 fixation, presumably due to attenuation, but not complete blockage, of the TCA-cycle.

Metabolite profiles of the *sucD* mutant and wild-type bacteroids (Figure 4) show that while succinate levels were similar in RU116 and wild-type bacteroids, fumarate and malate were considerably lower in the mutant bacteroids, indicating reduced flux of carbon. Our key question concerns the decarboxylating arm of the TCA-cycle. Predictably for a mutant strain blocked in the TCA-cycle at succinyl-CoA synthetase, citrate levels were 11-fold higher in *sucD* than wild-type and intermediates derived from 2-oxoglutarate, such as glutamate, glutathione and 2-hydroxyglutarate, were all increased markedly (Figure 4). Therefore, attenuation of succinyl-CoA synthetase activity caused an accumulation of metabolites prior to the decarboxylating arm of the TCA-cycle. Thus, the TCA-cycle operates in bacteroids and reducing its activity also reduced N_2-fixation. Crucially though, while the level of pyruvate was similar between the two bacteroid types, no acetyl-CoA and free Coenzyme A were detected in the *sucD* mutant. If the only major route for acetyl-CoA metabolism is the TCA-cycle, its levels should rise dramatically in strain RU116 (*sucD*). This suggests acetyl-CoA has other large sinks independent of the TCA-cycle. The presence of alternative sinks for acetyl-CoA would explain its very low level in bacteroids compared to free-living bacteria. It would also have profound implications for our understanding of *Rhizobium*-legume symbioses as it suggests a major re-routing of central metabolism during N_2 fixation in pea bacteroids.

Lipids are a sink for acetyl-CoA in bacteroids. Apart from its complete oxidation in the TCA-cycle, the other major metabolic fate of acetyl-CoA is in lipogenesis. Two possible products of lipogenesis are poly-β-hydroxybutyrate (PHB) and fatty acids. Considerable attention has focussed on PHB because it is abundant in soybean and common bean bacteroids, although it is thought to be absent from mature N_2-fixing bacteroids from indeterminate nodulating

403 plants including pea, alfalfa and clover. In contrast, there has been relatively little
404 quantification of bacteroid lipids, which we sought to address.
405
406 There was a range of chain lengths and degrees of unsaturation in the free-fatty acids in
407 both bacteroids and free-living succinate-grown cells (Table 2). Levels of long chain free-
408 fatty acids (C16-C20) were higher in bacteroids than in either free-living bacteria or nodule
409 cytosolic fractions. There were also significantly higher levels of monoacylglycerols, with
410 bacteroids containing highly elevated levels of 1-linoleoylglycerol (>57-fold), 1-
411 palmitoylglycerol (16-fold), 2-linoleoylglycerol (> 13-fold) as well as 1-stearoylglycerol (3.9-
412 fold) and 2-oleoylglycerol (5.8-fold). Moreover, the less efficient N_2-fixing *sucD* mutant
413 strain showed significantly lower levels of these lipid species compared to wild-type Rlv3841
414 bacteroids. The presence of these molecules at high levels in wild-type Rlv3841 suggests
415 bacteroids use fatty acids as a sink for acetyl-CoA.
416
417 It was not possible to detect diacyclglycerols or triacylglycerols in these samples as they fall
418 outside the polarity range and upper size limit of the GC- and LC-MS techniques used.
419 Therefore, membrane-free extracts were isolated by ultracentrifugation and their
420 glycerolipid level quantified by enzyme assay. Glycerolipids were 22-fold higher in
421 bacteroids than free-living cells (62 ± 2.66 ng/mg protein vs 2.8 ± 1.26 ng/mg protein,
422 respectively). Bacteroids channel a large proportion of acetyl-CoA away from the TCA-cycle
423 and into lipids, suggesting related storage mechanisms may be utilised under N_2-fixing
424 conditions.
425

426 **Pea bacteroids of Rlv3841 accumulate PHB.** PHB accumulation occurs in undifferentiated
427 rhizobia in infection threads of pea nodules but is thought to be absent in bacteroids (20).
428 When *R. leguminosarum* strain A34 was mutated in *phaC*, encoding a type I PHB synthase, it
429 lacked detectable PHB in both infection thread bacteria and in bacteroids. This is consistent
430 with the paradigm that bacteroids from indeterminate nodules such as pea and alfalfa do
431 not make PHB in bacteroids. However, the genome of *R. leguminosarum* strain Rlv3841 has
432 two PHB synthases: a type I on the chromosome (*phaC1,* RL2094) and a *phaE* (pRL100104)
433 *phaC2* (pRL100105) type II PHB synthase on the symbiotic plasmid pRL10. The putative
434 operon containing *phaEphaC2* is preceded by a consensus *nifA* promoter and was induced 7
435 to 40-fold in bacteroids, while *phaC1* was not upregulated (39). As PHB is another lipogenic
436 end-product of acetyl-CoA metabolism, we investigated the symbiotic roles of these two
437 PHB synthases in Rlv3841.
438
439 Previous work demonstrated that *phaC1* was active in free-living Rlv3841 as mutation of this
440 gene reduced PHB accumulation in the mutant RU137 by 93% relative to wild-type (12),
441 although the symbiotic performance of this *phaC1* mutant was not determined. Therefore,
442 we isolated a *phaC2* single mutant (LMB814) and a *phaC1 phaC2* double mutant (LMB816)
443 in Rlv3841 and assessed their symbiotic phenotype, along with the original *phaC1* mutant.
444 While rates of N_2 fixation in *phaC1, phaC2* single and *phaC1 phaC2* double mutants were not
445 significantly different from wild-type Rlv3841 (Supplementary Figure 1), examination of
446 nodule sections by TEM showed that PHB accumulation was altered. Pea nodules containing
447 wild-type Rlv3841 exhibited large PHB droplets in bacteria in infection threads and smaller
448 bodies in mature bacteroids (Figure 5). Previously when small PHB droplets were observed
449 in bacteroids it was assumed they were synthesized by bacteria in infection threads.

450 However, while the *phaC1* mutant harboured small PHB droplets in bacteroids, they were
451 absent in the undifferentiated bacteria in infection threads. Conversely, PHB was largely
452 absent in *phaC2* mutant bacteroids, but was abundant in bacteria occupying infection
453 threads. Finally, PHB was absent from both bacteroids and bacteria in infection threads in
454 the *phaC1 phaC2* mutant. Therefore, Rlv3841 has two functional PHB synthases: one active
455 in free-living and undifferentiated bacteria (type I, PhaC1) and the other in bacteroids (type
456 II, PhaE PhaC2). Although most sequenced rhizobia carry a type I PHB synthase, analysis of
457 genome sequences shows other rhizobia contain *phaEphaC2* genes, including strains
458 forming symbiotic interactions not usually thought to make PHB, such as *R. leguminosarum*
459 bv. viciae VF39 (pea) and *R. leguminosarum* bv. trifolii TA1 (clover) (Integrated Microbial
460 Genomes: https://img.jgi.doe.gov/cgi-bin/w/main.cgi). It is therefore likely that these other
461 type II-harbouring bacteroids also accumulate PHB, as has been demonstrated for Rlv3841.
462
463 **Discussion**
464 The metabolism of free-living Rlv3841 growing on succinate as the sole carbon source is
465 dominated by flux through the TCA-cycle as well as anaplerotic and biosynthetic reactions.
466 However, while the TCA-cycle is essential for fully effective N_2 fixation in pea bacteroids, the
467 accumulation of lipid shows a significant alternative fate for acetyl-CoA. Importantly, this
468 observation is supported by the work of Miller and Tremblay (48) who showed that *S.*
469 *meliloti* bacteroids from alfalfa nodules contain 34% of the total neutral lipid fraction as di-
470 and triglycerides, whereas these lipids were undetected in free-living *S. meliloti*. Moreover,
471 the extraordinary deposition of PHB in bacteroids from common bean and soybean is an
472 extreme example of carbon storage and redox balancing that has hitherto lacked a coherent
473 explanation, particularly since preventing synthesis in these symbioses does not prevent N_2

474 fixation (19-21). Here we show that bacteroids of some strains of *R. leguminosarum,* such as
475 Rlv3841, make PHB via a putative *nifA*-dependent type II PHB synthase. Therefore, the
476 paradigm that mature bacteroids from indeterminate nodules (such as those formed on
477 pea, alfalfa and clover) do not synthesize PHB is incorrect. Most importantly, Rlv3841
478 bacteroids accumulate both PHB and lipid showing that even with acetyl-CoA incorporated
479 into lipids, yet more acetyl-CoA accumulates in PHB. Thus, entry of acetyl-CoA into the TCA-
480 cycle must be limited and implies that symbiotic N_2 fixation should be thought of as a
481 fundamentally lipogenic process.
482
483 The complete oxidation of a mole of acetyl-CoA in the TCA cycle yields four moles of
484 reducing equivalents (i.e. NAD(P)H or $FADH_2$). In free-living rhizobia, this reductant can be
485 channelled to the aerobic respiratory chain, driving oxidative phosphorylation, or used as
486 reductant in biosynthesis to fuel cell growth and division. However, mature pea bacteroids
487 are in a metabolically active but non-dividing state. In addition, N_2 fixation in legume root
488 nodules occurs at microaerobic O_2 concentrations, estimated at 3 to 57 nM (49, 50). This
489 low O_2 level is likely to restrict bacteroid respiration and hence TCA cycle activity, thereby
490 forcing acetyl-CoA into lipids. While it is theoretically possible to have large rates of electron
491 flux to a high-affinity terminal oxidase such as *cbb*$_3$ in bacteroids if O_2-flux is also high, the
492 large scale production of lipids and PHB suggests this route is restricted. Instead, by
493 channelling acetyl-CoA into lipid and PHB synthesis, bacteroids could overcome this
494 metabolic constraint by consuming both carbon and reductant as NAD(P)H. Lipogenesis is a
495 classic response of all domains of life to an excess of carbon and reductant that cannot be
496 reoxidised by respiration or fermentation. Thus, free-living bacteria synthesise lipid when
497 growth is nutritionally unbalanced, such as in O_2- or N_2-limited conditions (51, 52). During

498 free-living N_2 fixation, both *Azotobacter beijerinckii* and *A. caulinodans* accumulate PHB and
499 in *A. caulinodans*, PHB synthesis is essential to both free-living and symbiotic N_2 fixation (22,
500 53). Thus, bacteroids may be lipogenic as a physiological response to the microaerobic
501 environment inside legume root nodules.
502
503 Although aerobically-growing free-living rhizobia and bacteroids differ in O_2 supply and
504 ability to divide, the other obvious metabolic difference is the supply of ATP and reductant
505 for bacteroid nitrogenase. Bacteroids must supply reductant and ATP to nitrogenase,
506 requiring 8 moles of electrons and 16 moles of ATP to reduce one mole of N_2 (Equation 1).
507 Although the electron source for nitrogenase is well understood in the free-living N_2-fixing
508 bacteria *Klebsiella pneumoniae,* where electrons are transferred by NifJ (pyruvate:flavin
509 oxidoreductase) and NifF (flavodoxin) complex from pyruvate to nitrogenase (54, 55), it is
510 unknown for rhizobia. In the classical model in rhizobia, all reductant generated by
511 metabolism, primarily as NAD(P)H, can be allocated to all processes including N_2 reduction
512 or biosynthesis with excess reductant and ATP consumed by lipogenesis (Figure 6).
513 However, the standard redox potentials of NADH and ferredoxin ($E^{0'}$ for NAD^+/NADH is -320
514 mV and ferredoxin Fe^{3+}/Fe^{2+} -is 484 mV (16, 17)), suggest it is unlikely that NADH donates
515 electrons directly to ferredoxin and then to nitrogenase. An alternative would be that a
516 specific molecule acts as the low potential electron donor to nitrogenase, such as pyruvate
517 oxidation by the NifJ-NifF complex in *K. pneumoniae* (54, 55). This process consumes four
518 pyruvate molecules and produces four acetyl-CoA to generate the eight electrons needed by
519 nitrogenase. Since this complex is not present in rhizobia, an alternative pathway is
520 required. One possibility is that the Electron Transferring Flavoprotein (ETF) complex,
521 FixABCX, interacts with pyruvate dehydrogenase, as shown by genetic suppressor analysis in

522 *A. caulinodans* (56). ETF complexes use electron bifurcation in anaerobic bacteria (57, 58),
523 which might enable FixABCX to generate low potential electrons for reduction of ferredoxin
524 and then N_2 (Figure 6). While unproven, such a mechanism requires eight moles of pyruvate
525 to reduce one mole of N_2 and would exacerbate the reductant problem because acetyl-CoA
526 oxidised by the TCA cycle would generate excess NAD(P)H. In the absence of convincing
527 experimental evidence for the electron donation pathway to nitrogenase, we cannot
528 complete a formal electron and reductant balance. However, Figure 6 illustrates how
529 dramatically redox balance in bacteroids can be altered by the need for low potential
530 electrons for N_2 reduction.
531
532 While *A. caulinodans,* must synthesize PHB during N_2 fixation (22), synthesis can be blocked
533 in bacteroids of peas, alfalfa, common bean and soybean (19-21, 59, 60). The ability to
534 prevent PHB synthesis and still have a functioning bacteroid may be explained by multiple
535 storage sinks for acetyl-CoA including PHB, free fatty acids, glycerolipids and membrane
536 phospholipids, with PHB itself being less important in these symbioses. Overall, bacteroids
537 are highly lipogenic, with multiple lipid sinks for excess reductant. This applies to both
538 determinate and indeterminate nodules and is likely to be an essential part of the
539 energisation of nitrogenase and associated redox balance in all N_2-fixing symbioses.
540
541
542

Acknowledgments

This work was supported by the Biotechnology and Biological Sciences Research Council [grant number BB/F013159/1]. We thank Drs Graham O'Hara and Garth Maker (Murdoch University, Australia) for valuable input in preparing this manuscript. The collaboration between Dr Jason Terpolilli and Professor Philip Poole is supported by Murdoch University through the Sir Walter Murdoch Adjunct Professor Scheme.

References

1. **Olivares J, Bedmar EJ, Sanjuan J.** 2013. Biological nitrogen fixation in the context of global change. Mol Plant-Microbe Interact **26:**486-494.
2. **Herridge DF, Peoples MB, Boddey RM.** 2008. Global inputs of biological nitrogen fixation in agricultural systems. Plant Soil **311:**1–18.
3. **Udvardi M, Poole PS.** 2013. Transport and metabolism in legume-rhizobia symbioses. Ann Rev Plant Biol **64:**781-805.
4. **Terpolilli JJ, Hood GA, Poole PS.** 2012. What determines the efficiency of N_2-fixing *Rhizobium*-legume symbioses? Adv Micro Phys **60:**325-389.
5. **Mulley G, Lopez-Gomez M, Zhang Y, Terpolilli J, Prell J, Finan T, Poole P.** 2010. Pyruvate is synthesized by two pathways in pea bacteroids with different efficiencies for nitrogen fixation. J Bacteriol **192:**4944-4953.
6. **Driscoll BT, Finan TM.** 1993. NAD^+-dependent malic enzyme of *Rhizobium meliloti* is required for symbiotic nitrogen fixation. Mol Microbiol **7:**865-873.
7. **Driscoll BT, Finan TM.** 1997. Properties of NAD^+- and $NADP^+$-dependent malic enzymes of *Rhizobium* (*Sinorhizobium*) *meliloti* and differential expression of their genes in nitrogen-fixing bacteroids. Microbiology **143:**489-498.

8. **Preisig O, Anthamatten D, Hennecke H.** 1993. Genes for a microaerobically induced oxidase complex in *Bradyrhizobium japonicum* are essential for a nitrogen-fixing endosymbiosis. Proc Natl Acad Sci USA **90:**3309-3313.

9. **Delgado MJ, Bedmar EJ, Downie JA.** 1998. Genes involved in the formation and assembly of rhizobial cytochromes and their role in symbiotic nitrogen fixation. Adv Micro Phys **40:**191-231.

10. **Mortimer MW, McDermott TR, York GM, Walker GC, Kahn ML.** 1999. Citrate synthase mutants of *Sinorhizobium meliloti* are ineffective and have altered cell surface polysaccharides. J Bacteriol **181:**7608-7613.

11. **Koziol U, Hannibal L, Rodriguez MC, Fabiano E, Kahn ML, Noya F.** 2009. Deletion of citrate synthase restores growth of *Sinorhizobium meliloti* 1021 aconitase mutants. J Bacteriol **191:**7581-7586.

12. **Walshaw DL, Wilkinson A, Mundy M, Smith M, Poole PS.** 1997. Regulation of the TCA cycle and the general amino acid permease by overflow metabolism in *Rhizobium leguminosarum*. Microbiology **143:**2209-2221.

13. **Pardo MA, Lagunez J, Miranda J, Martinez E.** 1994. Nodulating ability of *Rhizobium tropici* is conditioned by a plasmid-encoded citrate synthase. Mol Microbiol **11:**315-321.

14. **Green LS, Emerich DW.** 1997. The formation of nitrogen-fixing bacteroids is delayed but not abolished in soybean infected by an α-ketoglutarate dehydrogenase-deficient mutant of *Bradyrhizobium japonicum*. Plant Physiol **114:**1359-1368.

15. **Shah R, Emerich DW.** 2006. Isocitrate dehydrogenase of *Bradyrhizobium japonicum* is not required for symbiotic nitrogen fixation with soybean. J Bacteriol **188:**7600-7608.

592 16. **Carter KR, Rawlings J, Orme-Johnson WH, Becker RR, Evans HJ.** 1980. Purification
593 and characterization of a ferredoxin from *Rhizobium japonicum* bacteroids. J Biol
594 Chem **255:**4213-4223.
595 17. **Loach PA.** 2010. Oxidation-reduction potentials, absorbance bands and molar
596 absorbance of compounds used in biochemical studies, p 557-578. *In* Lundblad RL,
597 Macdonald F (ed), Handbook of Biochemistry and Molecular Biology. CRC Press, Boca
598 Raton.
599 18. **Sprent JI.** 2009. Legume Nodulation: A Global Perspective. Wiley-Blackwell, Oxford.
600 19. **Cevallos MA, Encarnacion S, Leija A, Mora Y, Mora J.** 1996. Genetic and
601 physiological characterization of a *Rhizobium etli* mutant strain unable to synthesize
602 poly-beta-hydroxybutyrate. J Bacteriol **178:**1646-1654.
603 20. **Lodwig EM, Leonard M, Marroqui S, Wheeler TR, Findlay K, Downie JA, Poole PS.**
604 2005. Role of polyhydroxybutyrate and glycogen as carbon storage compounds in
605 pea and bean bacteroids. Mol Plant-Microbe Interact **18:**67-74.
606 21. **Quelas JI, Mongiardini EJ, Perez-Gimenez J, Parisi G, Lodeiro AR.** 2013. Analysis of
607 two polyhydroxyalkanoate synthases in *Bradyrhizobium japonicum* USDA 110. J
608 Bacteriol **195:**3145-3155.
609 22. **Mandon K, Michel-Reydellet N, Encarnacion S, Kaminski PA, Leija A, Cevallos MA,**
610 **Elmerich C, Mora J.** 1998. Poly-β-hydroxybutyrate turnover in *Azorhizobium*
611 *caulinodans* is required for growth and affects *nifA* expression. J Bacteriol **180:**5070-
612 5076.
613 23. **Beringer JE.** 1974. R factor transfer in *Rhizobium leguminosarum*. J Gen Microbiol
614 **84:**188-198.

615 24. **Poole PS, Schofield NA, Reid CJ, Drew EM, Walshaw DL.** 1994. Identification of
616 chromosomal genes located downstream of *dctD* that affect the requirement for
617 calcium and the lipopolysaccharide layer of *Rhizobium leguminosarum*. Microbiology
618 **140:**2797-2809.
619 25. **Masakapalli SK, Kruger NJ, Ratcliffe RG.** 2013. The metabolic flux phenotype of
620 heterotrophic *Arabidopsis* cells reveals a complex response to changes in nitrogen
621 supply. Plant J **74:**569-582.
622 26. **Kruger NJ, Masakapalli SK, Ratcliffe RGJ.** 2012. Strategies for investigating the plant
623 metabolic network with steady-state metabolic flux analysis: lessons from an
624 *Arabidopsis* cell culture and other systems. J Exp Bot **63**.
625 27. **Lawton KA, Berger A, Mitchell M, Milgram KE, Evans AM, Guo L, Hanson RW,**
626 **Kalhan SC, Ryals JA, Milburn MV.** 2008. Analysis of the adult human plasma
627 metabolome. Pharmacogenomics **9:**383-397.
628 28. **Evans AM, DeHaven CD, Barrett T, Mitchell M, Milgram E.** 2009. Integrated,
629 nontargeted ultrahigh performance liquid chromatography/electrospray ionization
630 tandem mass spectrometry platform for the identification and relative quantification
631 of the small-molecule complement of biological systems. Anal Chem **81:**6656-6667.
632 29. **Yobi A, Wone BW, Xu W, Alexander DC, Guo L, Ryals JA, Oliver MJ, Cushman JC.**
633 2012. Comparative metabolic profiling between desiccation-sensitive and
634 desiccation-tolerant species of *Selaginella* reveals insights into the resurrection trait.
635 Plant J **72:**983-999.
636 30. **Bradford MM.** 1976. A rapid and sensitive method for the quantitation of microgram
637 quantities of protein utilizing the principle of protein-dye binding. Anal Biochem
638 **72:**248-254.

639 31. **Storey JD, Tibshirani R.** 2003. Statistical significance for genomewide studies. Proc
640 Natl Acad Sci USA **100:**9440-9445.
641 32. **Yates RJ, Howieson JG, Hungria M, Bala A, O'Hara GW, Terpolilli JJ.** 2016.
642 Authentication of rhizobia and assessment of the legume symbiosis in controlled
643 plant growth systems, p 73-108. *In* Howieson JG, Dilworth MJ (ed), Working with
644 rhizobia. Australian Centre for International Agricultural Research, Canberra.
645 33. **Allaway D, Lodwig EM, Crompton LA, Wood M, Parsons R, Wheeler TR, Poole PS.**
646 2000. Identification of alanine dehydrogenase and its role in mixed secretion of
647 ammonium and alanine by pea bacteroids. Mol Microbiol **36:**508-515.
648 34. **Buchanan-Wollaston V.** 1979. Generalized transduction in *Rhizobium*
649 *leguminosarum*. J Gen Microbiol **112**.
650 35. **Lodwig E, Poole P.** 2003. Metabolism of *Rhizobium* bacteroids. Crit Rev Plant Sci
651 **22:**37-78.
652 36. **Joy KW, Prabha C.** 1986. The role of transamination in the synthesis of homoserine
653 in peas. Plant Physiol **82:**99-102.
654 37. **Prell J, Bourdes A, Karunakaran R, Lopez-Gomez M, Poole P.** 2009. Pathway of γ-
655 aminobutyrate metabolism in *Rhizobium leguminosarum* 3841 and its role in
656 symbiosis. J Bacteriol **191:**2177-2186.
657 38. **Min B, Pelaschier JT, Graham DE, Tumbula-Hansen D, Soll D.** 2002. Transfer RNA-
658 dependent amino acid biosynthesis: an essential route to asparagine formation. Proc
659 Natl Acad Sci U S A **99:**2678-2683.
660 39. **Karunakaran R, Ramachandran VK, Seaman JC, East AK, Mouhsine B, Mauchline**
661 **TH, Prell J, Skeffington A, Poole PS.** 2009. Transcriptomic analysis of *Rhizobium*

leguminosarum biovar viciae in symbiosis with host plants *Pisum sativum* and *Vicia cracca*. J Bacteriol **191:**4002-4014.

40. **Vanderlinde EM, Hynes MF, Yost CK.** 2014. Homoserine catabolism by *Rhizobium leguminosarum* bv. viciae 3841 requires a plasmid-borne gene cluster that also affects competitiveness for nodulation. Environ Microbiol **16:**205-217.

41. **Huerta-Zepeda A, Ortuno L, Du Pont G, Duran S, Lloret A, Merchant-Larios H, Calderon J.** 1997. Isolation and characterization of *Rhizobium etli* mutants altered in degradation of asparagine. J Bacteriol **179:**2068-2072.

42. **McKay IA, Dilworth MJ, Glenn AR.** 1989. Carbon catabolism in continuous cultures and bacteroids or *Rhizobium leguminosarum* MNF3841. Arch Microbiol **152:**606-610.

43. **Tabrett CA, Copeland L.** 2000. Biochemical controls of citrate synthase in chickpea bacteroids. Arch Microbiol **173:**42-48.

44. **Dunn MF.** 1998. Tricarboxylic acid cycle and anaplerotic enzymes in rhizobia. FEMS Microbiol Rev **22:**105-123.

45. **Patriarca EJ, Tate R, Iaccarino M.** 2002. Key role of bacterial NH_4^+ metabolism in *Rhizobium*-plant symbiosis. Microbiol Mol Biol Rev **66:**203-222.

46. **Mulley G, White JP, Karunakaran R, Prell J, Bourdes A, Bunnewell S, Hill L, Poole PS.** 2011. Mutation of GOGAT prevents pea bacteroid formation and N_2 fixation by globally downregulating transport of organic nitrogen sources. Mol Microbiol **80:**149-167.

47. **Poole P, Reid C, East AK, Allaway D, Day M, Leonard M.** 1999. Regulation of the *mdh-sucCDAB* operon in *Rhizobium leguminosarum*. FEMS Microbiol Lett **176:**247-255.

48. **Miller RW, Tremblay PA.** 1983. Cytoplasmic membrane of *Rhizobium meliloti* bacteroids. I. Alterations in lipid composition, physical properties, and respiratory proteins. Can J Biochem Cell Biol **61:**1334-1340.

49. **Kuzma MM, Hunt S, Layzell DB.** 1993. Role of oxygen in the limitation and inhibition of nitrogenase activity and respiration rate in individual soybean nodules. Plant Physiol **101:**161-169.

50. **Appleby CA.** 1984. Leghaemoglobin and *Rhizobium* respiration. Ann Rev Plant Physiol **35:**443-478.

51. **Rehm BH.** 2010. Bacterial polymers: biosynthesis, modifications and applications. Nat Rev Microbiol **8:**578-592.

52. **Waltermann M, Steinbuchel A.** 2005. Neutral lipid bodies in prokaryotes: recent insights into structure, formation, and relationship to eukaryotic lipid depots. J Bacteriol **187:**3607-3619.

53. **Senior PJ, Beech GA, Ritchie GA, Dawes EA.** 1972. The role of oxygen limitation in the formation of poly-β-hydroxybutyrate during batch and continuous culture of *Azotobacter beijerinckii*. Biochem J **128:**1193-1201.

54. **Shah VK, Stacey G, Brill WJ.** 1983. Electron transport to nitrogenase. Purification and characterization of pyruvate:flavodoxin oxidoreductase. The *nifJ* gene product. J Biol Chem **258:**12064-12068.

55. **Nieva-Gomez D, Roberts GP, Klevickis S, Brill WJ.** 1980. Electron transport to nitrogenase in *Klebsiella pneumoniae*. Proc Natl Acad Sci USA **77:**2555-2558.

56. **Scott JD, Ludwig RA.** 2004. *Azorhizobium caulinodans* electron-transferring flavoprotein N electrochemically couples pyruvate dehydrogenase complex activity to N_2 fixation. Microbiology **150:**117-126.

Journal of Bacteriology

57. **Bertsch J, Parthasarathy A, Buckel W, Muller V.** 2013. An electron-bifurcating caffeyl-CoA reductase. J Biol Chem **16:**11304-11311.

58. **Hess V, Gonzalez JM, Parthasarathy A, Buckel W, Muller V.** 2013. Caffeate respiration in the acetogenic bacterium *Acetobacterium woodii*: a coenzyme A loop saves energy for caffeate activation. Appl Environ Microbiol **79:**1942-1947.

59. **Povolo S, Tombolini R, Morea A, Anderson AJ, Casella S, Nuti MP.** 1994. Isolation and characterization of mutants of *Rhizobium meliloti* unable to synthesize poly-β-hydroxybutyrate. Can J Microbiol **40:**823-829.

60. **Aneja P, Charles TC.** 1999. Poly-3-hydroxybutyrate degradation in *Rhizobium* (*Sinorhizobium*) *meliloti*: isolation and characterization of a gene encoding 3-hydroxybutyrate dehydrogenase. J Bacteriol **181:**849-857.

61. **Johnston AWB, Beringer JE.** 1975. Identification of the *Rhizobium* strains in pea root nodules using genetic markers. J Gen Microbiol **87:**343-350.

62. **Prentki P, Krisch HM.** 1984. In vitro insertional mutagenesis with a selectable DNA fragment. Gene **29:**303-313.

63. **Quandt J, Hynes MF.** 1993. Versatile suicide vectors which allow direct selection for gene replacement in Gram-negative bacteria. Gene **127:**15-21.

64. **Figurski DH, Helinski DR.** 1979. Replication of an origin-containing derivative of plasmid RK2 dependent on a plasmid function provided *in trans*. Proc Natl Acad Sci USA **76:**1648-1652.

65. **Karunakaran R, Haag AF, East AK, Ramachandran VK, Prell J, James EK, Scocchi M, Ferguson GP, Poole PS.** 2010. BacA is essential for bacteroid development in nodules of galegoid, but not phaseoloid, legumes. J Bacteriol **192:**2920-2928.

732 **Table 1 –** Strains, plasmids and primers used in this study.

Strain, Plasmid or Primer	Genotype or Sequence	Reference
Strains		
Rlv3841	St^r derivative of *R. leguminosarum* bv. *viciae* strain 300	(61)
RU137	Rlv3841 *phaC1*::Tn*5*; Nm^r	(12)
RU116	Rlv3841 *sucD*::Tn*5*; Nm^r	(12)
RU156	Rlv3841 *sucA*::Tn*5*; Nm^r	(12)
RU724	Rlv3841 *sucA*::Tn*5-lacZ* ; Nm^r	(12)
RU725	Rlv3841 *sucC*::Tn*5-lacZ* ; Nm^r	(12)
RU726	Rlv3841 *sucB*::Tn*5-lacZ*; Nm^r	(12)
RU733	Rlv3841 *sucA*::Tn*5-lacZ*; Nm^r	(12)
LMB814	Rlv3841 *phaC2*::Ω; St^r Sp^r	This work
LMB816	Rlv3841 *phaC1*::Tn5 *phaC2*::Ω; St^r Nm^r Sp^r	This work
DH5α	*Escherichia coli* strain used for cloning: F$^-$ *ϕ80lacZΔM15* Δ*(lacZYA-argF) U169 recA1 endA1 hsdR17*(r_k^-, m_k^+) *phoA supE44 thi-1gyrA96 relA1*	Invitrogen
Plasmids		
pJET1.2/Blunt	PCR product cloning vector; Ap^r	Thermo-Fisher
pHP45-ΩSmSp	pHP derivative with ΩSmSp cassette, Sm^r Sp^r	(62)
pJQ200SK	pACYC derivative, P15A origin of replication insertional mutagenesis inactivation vector, Gm^r Suc^s	(63)
pRK2013	Helper plasmid used for mobilizing plasmids. ColE1 replicon with RK2 *tra* genes, Km^r	(64)
pLMB834	pr1645-1646 PCR product (2.8 kbp) from pRL100105 (*phaC2*) cloned into pJET1.2/Blunt, Ap^r	This work
pLMB835	pLMB834 with ΩSmSp cassette from pHP45-ΩSmSp cloned into unique EcoRI site, Ap^r Sm^r Sp^r	This work
pLMB838	pJQ200SK with BglII fragment from pLMB835 containing *phaC2*:: Ω cloned into BamH1 site, Sm^r Sp^r Gm^r Suc^s	This work
Primers		
pr1645	AACGCTACAGCGCAACGCTC	This work
pr1646	ACTTTCTTCGCTCCCGTCGG	This work
pr1647	ACCCCGAAGACGCTCGTCAT	This work
pr1648	ATGATCGTGACGGCATCGGC	This work
potfarforward	GACCTTTTGAATGACCTTTA	(65)
Tn5-1	ATAGCCTCTCCACCCAAGC	This work

733

734 **Table 2** – Comparison of fatty acids and monoacylglycerols detected in metabolite profiles
735 showing the fold change in metabolite abundance, in Rlv3841 bacteroids relative to Rlv3841
736 free-living, nodule cytosol and *sucD* bacteroid samples, respectively. Boxes highlighted in
737 red were significantly higher ($P < 0.05$ and $Q < 0.1$) and those in green were significantly
738 lower ($P<0.05$ and $Q<0.1$) in Rlv3841 bacteroids, with un-highlighted boxes showing no
739 significant difference.

	Fold Change in Metabolite Abundance (Amount in Rlv3841 bacteroids relative to other sample)		
Lipid Species	**Rlv3841 Bacteroids *vs.* Rlv3841 Free-living**	**Rlv3841 Bacteroids *vs.* Nodule cytosol**	**Rlv3841 Bacteroids *vs.* *sucD* Bacteroids**
Free Fatty Acids			
cis-vaccenate (18:1n7)	**1.99**	**5.91**	**4.00**
palmitoleate (16:1n7)	**8.20**	**4.87**	**2.94**
linolenate [α or γ (18:3n3 or 6)]	**23.0**	**4.09**	1.32
linoleate (18:2n6)	**18.7**	**3.62**	**2.13**
eicosenoate (20:1n9 or 11)	**8.39**	**2.91**	**2.56**
10-heptadecenoate (17:1n7)	**8.22**	**2.54**	1.19
dihomo-linoleate (20:2n6)	**3.81**	**2.50**	1.28
stearate (18:0)	**2.16**	**1.90**	**2.44**
palmitate (16:0)	**3.72**	**1.88**	**2.94**
margarate (17:0)	**3.94**	1.15	**1.89**
pelargonate (9:0)	0.75	**0.48**	**2.17**
heptanoate (7:0)	**0.19**	**0.19**	**0.46**
caproate (6:0)	**19.7**	**0.16**	0.71
caprylate (8:0)	1.45	**0.16**	0.75
isovalerate	1.30	**0.05**	**0.36**
Glycerolipids			
1-linoleoylglycerol (18:2)	**57.2**	**8.04**	**9.09**
2-linoleoylglycerol (18:2)	**13.2**	**5.38**	**6.25**
2-oleoylglycerol (18:1)	**5.83**	**3.16**	**2.78**
1-stearoylglycerol (18:0)	**3.86**	**0.33**	**3.85**
1-palmitoylglycerol (16:0)	**15.6**	**0.27**	**4.35**

740 **Figure 1 -** Flux map of central carbon metabolism for free-living *R. leguminosarum* Rlv3841,
741 grown on succinate and NH_4Cl. Net fluxes are expressed on a molar basis relative to
742 succinate uptake. The thickness of each arrow is proportional to net flux with the exception
743 that fluxes < 1% of succinate uptake are indicated by broken arrows. Biosynthetic outputs
744 are shown in solid rectangular boxes and metabolites treated as a single pool in the model
745 are shown in dashed grey boxes. Flux identifiers, defined in Supplementary Table 2, are
746 shown in italics. The precise values for the deduced fluxes are presented in Supplementary
747 Table 4. Standard abbreviations are used for amino acids and metabolic intermediates, and
748 PPP represent the reversible non-oxidative steps of the pentose phosphate pathway.
749
750 **Figure 2 -** Metabolite profile of Rlv3841 bacteroids *vs*. Rlv3841 free-living cells showing fold
751 change in metabolite abundance relative to Rlv3841 bacteroids. Bacteroids were isolated
752 from nodules from pea plants 28 days post-inoculation (dpi). Cells were harvested from log
753 phase cultures grown in AMS broth with 20 mM succinate and 10 mM NH_4Cl as the carbon
754 and nitrogen sources, respectively. Bolded intermediates were detected by metabolite
755 profiling, with a statistically significant fold difference ($P < 0.05$ by Welch's T-test and $Q < 0.1$
756 for the False Discovery Rate) denoted with a red (increase) or green (decrease) arrow. A >
757 sign indicates the metabolite was undetectable in either the free-living or the bacteroid
758 sample, so the difference reported is therefore a lower limit estimate of the fold change.
759 Intact arrows indicate single step enzyme catalysed reactions. Broken arrows indicate where
760 two or more enzyme-catalysed steps are involved in a series of reactions. Abbreviations: UD,
761 undetectable; BT, bacteroid; FL, free-living; GABA, γ-amino butyric acid; GSH, glutathione
762 (reduced); GSSG, glutathione (oxidised); 2OG, 2-oxoglutarate; OAA, oxaloacetate; PEP,
763 phosphoenolpyruvate.

764 **Figure 3** – Symbiotic phenotype of *sucD* mutant (RU116) compared to wild-type Rlv3841. N_2
765 fixation as measured by acetylene reduction on whole plants at 28 dpi expressed on (a) per
766 plant basis (n=6 per treatment) and (b) per unit bacteroid protein basis (n=6), where the
767 significance value $*P < 0.05$ was determined by Welch's T-test. A photograph of pea plants
768 (c) at 47 dpi with uninoculated water control (WC), Rlv3841 and *sucD* (RU116) treatments.
769 Mean shoot dry weights (d) of 42 dpi peas (n = 12 per treatment), where treatments not
770 sharing a letter differ significantly at $P < 0.05$ (ANOVA and Tukey's HSD). In all cases, error
771 bars represent standard errors of the means.
772
773 **Figure 4 -** Metabolite profile of *sucD* (RU116) bacteroids *vs*. Rlv3841 bacteroids showing fold
774 change in metabolite abundance relative to *sucD* bacteroids. Bacteroids were isolated from
775 nodules from pea plants 28 dpi. Bolded intermediates were detected by metabolite
776 profiling, with a statistically significant fold difference ($P < 0.05$ by Welch's T-test and $Q < 0.1$
777 for the False Discovery Rate) denoted with a red (increase) or green (decrease) arrow. Intact
778 arrows indicate single step enzyme catalysed reactions. Broken arrows indicate where two
779 or more enzyme-catalysed steps are involved in a series of reactions. *sucD* bacteroids are
780 attenuated in TCA-cycle enzymes post 2-oxoglutarate (2-OG). Abbreviations: UD,
781 undetectable; GABA, γ-amino butyric acid; GSH, glutathione (reduced); GSSG, glutathione
782 (oxidised); OAA, oxaloacetate; PEP, phosphoenolpyruvate.
783
784 **Figure 5 –** Transmission electron micrographs of pea nodules at 28 dpi. Wild-type Rlv3841
785 (a) bacteroids and (b) in an infection thread, both showing PHB droplets. Mutant *phaC1*
786 (RU137) (c) bacteroids showing PHB accumulation, which is absent from (d) infection
787 threads. Mutant *phaC2* (LMB814) (e) bacteroids where PHB droplets are largely absent, but

788 abundant in (f) in infection threads. Double mutant *phaC1 phaC2* (LMB816) (g) bacteroids
789 and (h) in infection threads with PHB absent from both. Scale bars are 2 µm in a, c, e and g
790 and 1 µm in b, d, f and h. Red arrows point to PHB droplets which appear white.
791
792 **Figure 6** – Two possible pathways of electron allocation in N_2-fixing bacteroids. (a) In the
793 first scenario, NADH supplies electrons directly to nitrogenase as well as providing ATP from
794 oxidative phosphorylation. A minimum of two moles of malate are required to be oxidised
795 to acetyl CoA to yield sufficient ATP and electrons to reduce one mole of N_2. (b) In the
796 second scenario, electrons are supplied to nitrogenase via a tight coupling with PDH and
797 electron bifurcation through FixABCX, requiring eight moles of malate to reduce one mole of
798 N_2. The 16 moles of electrons liberated from the oxidation of eight moles of pyruvate could
799 undergo electron bifurcation at FixABCX, resulting in eight electrons reducing CoQ via the
800 Fix complex, while eight electrons are channelled to nitrogenase and N_2 fixation. The 16 ATP
801 for N_2 fixation could be supplied from oxidative phosphorylation, for example the 8
802 electrons from FixABCX (i.e. $CoQH_2$) plus reoxidation of 8 $FADH_2$ generated in the TCA cycle.
803 However, in this scheme if all eight acetyl CoA are oxidised in the TCA cycle, then the large
804 yield of reductant (24 NADH plus the eight NADH from oxidation of malate by malic enzyme)
805 could result in over-reduction of the electron carrier pool, requiring bacteroids to consume
806 reductant and acetyl CoA through lipogenesis. The two models are not mutually exclusive as
807 in (a), free NADH might also interact with FixABCX enabling low potential electrons to be
808 generated by bifurcation for reduction of ferredoxin. Note that a P:$2e^-$ ratio of 2.5 is
809 assumed for NADH and 1.5 for electrons entering the ETC at the level of CoQ. For simplicity
810 we have not distinguished between NAD^+ and $NADP^+$ in this model. Abbreviations: CoQ,

811 Coenzyme Q; ETC, electron transport chain; ME, malic enzyme; N2ase, nitrogenase; PDH,

812 pyruvate dehydrogenase.

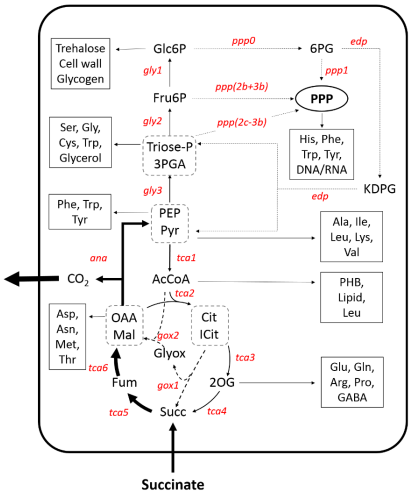

Figure 1.

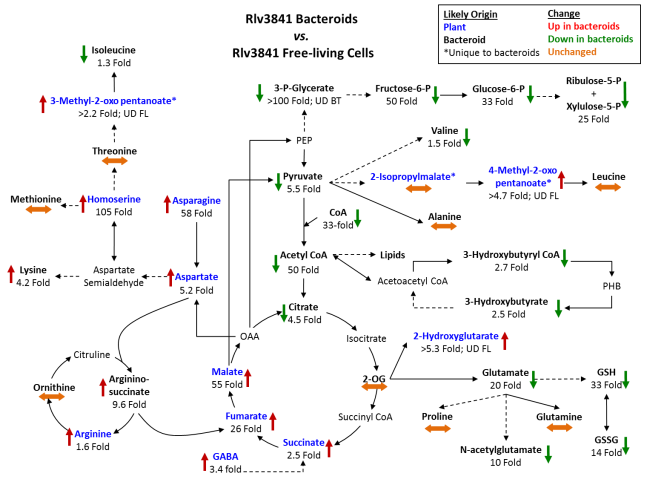

Figure 2.

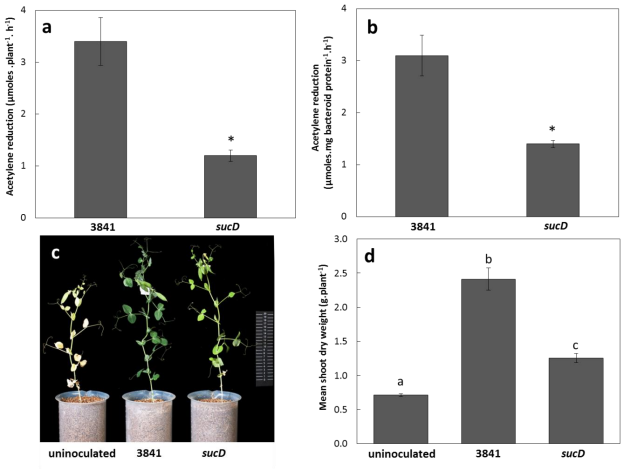

Figure 3

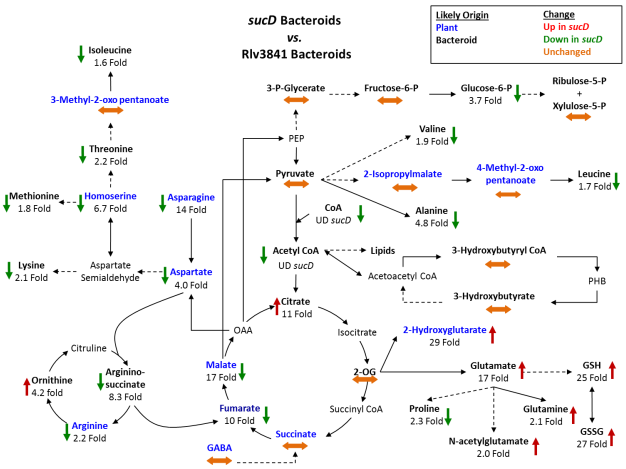

Figure 4

Figure 5

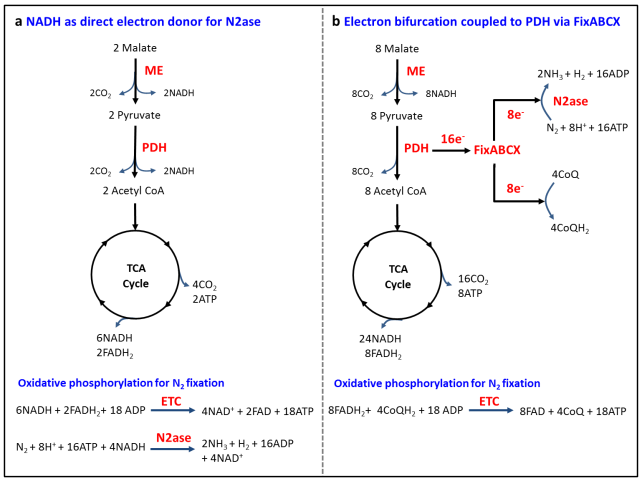

Figure 6